Majorana et al. *Journal of Mathematics in Industry* (2017) 7:4
DOI 10.1186/s13362-016-0027-3

Journal of Mathematics in Industry
a SpringerOpen Journal

RESEARCH Open Access

Charge transport and mobility in monolayer graphene

Armando Majorana[1], Giovanni Mascali[2] and Vittorio Romano[1*]

*Correspondence:
romano@dii.unict.it
[1]Dipartimento di Matematica e Informatica, Università di Catania, Viale A. Doria 6, Catania, 95125, Italy
Full list of author information is available at the end of the article

Abstract
For electron devices that make use of innovative materials, a basic step in the development of models and simulation computer aided design (CAD) tools is the determination of the mobility curves for the charge carriers. These can be obtained from experimental data or by directly solving the electron semiclassical Boltzmann equation. Usually the numerical solutions of the transport equation are obtained by Direct Simulation Monte Carlo (DSMC) approaches with the unavoidable stochastic noise due to the statistical fluctuations. Here we derive the mobility curves numerically solving the electron semiclassical Boltzmann equation with a deterministic method based on a discontinuous Galerkin (DG) scheme in the case of monolayer graphene. Comparisons with analytical mobility formulas are presented.

MSC: 82D37; 82C70; 82C80

Keywords: graphene; mobility; Boltzmann equation; discontinuous Galerkin method

1 Introduction

Graphene is a gapless semiconductor made of a single layer of carbon atoms arranged into a honeycomb hexagonal lattice [1]. In view of applications in graphene-based electron devices, it is crucial understanding the basic transport properties of this material.

An important step in the analysis of the electrical features of graphene is the determination of the mobility curves that can then be inserted in the simulation CAD tools already available for several semiconductor materials, e.g. Silicon and GaAs. The mobilities are functions of the electric field and depend also on factors like Fermi level, temperature and presence of impurities. The direct way to determine the mobility curves is by experiments. However the measurements are rather delicate and very sensible to the specific specimen one is dealing with. In particular the determination of the low field mobility is subject to a rather wide uncertainty, for example see [2] for Silicon.

An indirect theoretical way is instead based on the solutions of the transport equation; in fact once the distribution of electrons has been obtained, one can evaluate the current as a suitable average quantity.

Usually the numerical solutions of the transport equation are obtained by DSMC approaches with the unavoidable stochastic noise due to the statistical fluctuations. Here, in the case of monolayer graphene, we derive the mobility curves numerically solving the electron semiclassical Boltzmann equation with a deterministic DG method [3, 4]. At last

Springer

© 2016 Majorana et al. This article is distributed under the terms of the Creative Commons Attribution 4.0 International License (http://creativecommons.org/licenses/by/4.0/), which permits unrestricted use, distribution, and reproduction in any medium, provided you give appropriate credit to the original author(s) and the source, provide a link to the Creative Commons license, and indicate if changes were made.

the numerically obtained mobility is fitted with some analytical formulas which are widely used for other semiconductors such as Si or ZnO.

A remarkable point is that the low field mobility is obtained without the intrinsic huge noise in DSMC simulation at very low electric fields.

The plan of the paper is as follows. In Section 2 the transport equation for charge carriers in graphene is presented along with the derivation of the mobility expressions from the electron distribution functions. In Section 3 we illustrate the DG method for solving the Boltzmann equation and in the last section the numerical results of the mobilities are shown and fitted with analytical expressions.

2 Semiclassical transport equation for graphene and mobilities

The electron energy in graphene depends on a two dimensional wave-vector $\mathbf{k}$ belonging to a bi-dimensional Brillouin zone $\mathcal{B}$ which has a hexagonal shape.

Most of the electrons are in the valleys around the vertices of the Brillouin zone, called Dirac points or K and K' points. Usually the K and K' valleys are treated as a single equivalent one.

In a semiclassical kinetic setting, the charge transport in graphene is described by four Boltzmann equations, one for electrons in the valence band (π) and one for electrons in the conduction band (π^*), that in turn can belong to the K or K' valley,

$$\frac{\partial f_{\ell,s}(\mathrm{t},\mathbf{x},\mathbf{k})}{\partial \mathrm{t}} + \mathbf{v}_{\ell,s} \cdot \nabla_{\mathbf{x}} f_{\ell,s}(\mathrm{t},\mathbf{x},\mathbf{k}) - \frac{e}{\hbar}\mathbf{E} \cdot \nabla_{\mathbf{k}} f_{\ell,s}(\mathrm{t},\mathbf{x},\mathbf{k}) = \left.\frac{df_{\ell,s}}{d\mathrm{t}}(\mathrm{t},\mathbf{x},\mathbf{k})\right|_{e-ph}, \tag{1}$$

where $f_{\ell,s}(\mathrm{t},\mathbf{x},\mathbf{k})$ represents the distribution function of charge carriers, in the band π or π^* ($s = -1$ or $s = 1$) and valley ℓ (K or K'), at position $\mathbf{x}$, time t, and with wave-vector $\mathbf{k}$. We denote by $\nabla_{\mathbf{x}}$ and $\nabla_{\mathbf{k}}$ the gradients with respect to the position and the wave-vector, respectively. The group velocity $\mathbf{v}_{\ell,s}$ is related to the band energy $\varepsilon_{\ell,s}$ by

$$\mathbf{v}_{\ell,s} = \frac{1}{\hbar}\nabla_{\mathbf{k}}\varepsilon_{\ell,s}.$$

With a very good approximation [1] a linear dispersion relation holds for the band energies $\varepsilon_{\ell,s}$ around the equivalent Dirac points; so that $\varepsilon_{\ell,s} = s\hbar v_F|\mathbf{k} - \mathbf{k}_\ell|$, where v_F is the (constant) Fermi velocity, $\hbar$ the Planck constant divided by 2π, and $\mathbf{k}_\ell$ is the position of the Dirac point ℓ. The elementary (positive) charge is denoted by e, and $\mathbf{E}$ is the electric field, here assumed as external. The right hand sides of Eqs. (1) are the collision terms representing the interactions of electrons with acoustic, optical (with wave-vector close to the Γ point of the first Brillouin zone) and K phonons (with wave-vector close to the zone edge of the first Brillouin zone). Acoustic phonon scattering is intra-valley and intra-band. Optical phonon scattering is intra-valley and can be longitudinal optical (LO) and transversal optical (TO); it can be intra-band, leaving the electrons in the same band, or inter-band, pushing the electrons from the initial band toward another one. Scattering with optical phonons of K type pushes electrons from a valley to a nearby one (inter-valley scattering). We assume that phonons are a bath at thermal equilibrium. Hence, the general form of the collision

term can be written as (see [1, 5, 6] for more details)

$$\frac{df_{\ell,s}}{dt}(\mathrm{t},\mathbf{x},\mathbf{k})\Big|_{e-ph} = \sum_{\ell',s'}\Big[\int_{\mathcal{B}} S_{\ell',s',\ell,s}(\mathbf{k}',\mathbf{k}) f_{\ell',s'}(\mathrm{t},\mathbf{x},\mathbf{k}')\big(1-f_{\ell,s}(\mathrm{t},\mathbf{x},\mathbf{k})\big)\,d\mathbf{k}' \\ - \int_{\mathcal{B}} S_{\ell,s,\ell',s'}(\mathbf{k},\mathbf{k}') f_{\ell,s}(\mathrm{t},\mathbf{x},\mathbf{k})\big(1-f_{\ell',s'}(\mathrm{t},\mathbf{x},\mathbf{k}')\big)\,d\mathbf{k}'\Big],$$

where the total transition rate $S_{\ell',s',\ell,s}(\mathbf{k}',\mathbf{k})$ is given by the sum of the contributions of the several types of scatterings described above

$$S_{\ell',s',\ell,s}(\mathbf{k}',\mathbf{k}) = \sum_{\nu}\big|G^{(\nu)}_{\ell',s',\ell,s}(\mathbf{k}',\mathbf{k})\big|^2\Big[\big(n^{(\nu)}_{\mathbf{q}}+1\big)\delta\big(\varepsilon_{\ell,s}(\mathbf{k})-\varepsilon_{\ell',s'}(\mathbf{k}')+\hbar\omega^{(\nu)}_{\mathbf{q}}\big) \\ + n^{(\nu)}_{\mathbf{q}}\delta\big(\varepsilon_{\ell,s}(\mathbf{k})-\varepsilon_{\ell',s'}(\mathbf{k}')-\hbar\omega^{(\nu)}_{\mathbf{q}}\big)\Big]. \tag{2}$$

The index ν labels the νth phonon mode. The $|G^{(\nu)}_{\ell',s',\ell,s}(\mathbf{k}',\mathbf{k})|^2$'s are the electron-phonon coupling matrix elements, which describe the interaction mechanism of an electron with a ν-phonon, from the state of wave-vector $\mathbf{k}'$ belonging to the valley ℓ' and band s' to the state $\mathbf{k}$ belonging to the valley ℓ and band s. The symbol δ denotes the Dirac distribution, $\omega^{(\nu)}_{\mathbf{q}}$ is the νth phonon frequency, $n^{(\nu)}_{\mathbf{q}}$ is the Bose-Einstein distribution for the ν-type phonons

$$n^{(\nu)}_{\mathbf{q}} = \frac{1}{e^{\hbar\omega^{(\nu)}_{\mathbf{q}}/k_B T}-1}, \tag{3}$$

where k_B is the Boltzmann constant and T the graphene lattice temperature. If, for a ν_*-type phonon, $\hbar\omega^{(\nu_*)}_{\mathbf{q}} \ll k_B T$, then the corresponding scattering can be assumed elastic. In this case, we eliminate in Eq. (2) the term $\hbar\omega^{(\nu_*)}_{\mathbf{q}}$ inside the delta distribution and we use the Laurent approximation $n^{(\nu_*)}_{\mathbf{q}} \approx k_B T/\hbar\omega^{(\nu_*)}_{\mathbf{q}} - \frac{1}{2} + O(\hbar\omega^{(\nu_*)}_{\mathbf{q}}/k_B T)$.

It is preferable to treat the electrons in the valence band as holes for insuring the integrability of the corresponding distribution function. However, in this paper we consider the case of a high value of the Fermi energy, which is equivalent for conventional semiconductors to a n-type doping. Under such a condition, electrons belonging to the conduction band do not move to the valence band and vice versa. Therefore the hole dynamics is neglected. A reference frame centered in the K-point will be used and in order to simplify the notation the indices s and ℓ will be omitted.

Under the above hypotheses the scattering rates read as follows.

For acoustic phonons, we consider the elastic approximation according to which

$$\big(2n^{(ac)}_{\mathbf{q}}+1\big)\big|G^{(ac)}(\mathbf{k}',\mathbf{k})\big|^2 = \frac{1}{(2\pi)^2}\frac{\pi D^2_{ac} k_B T}{2\hbar\sigma_m v_p^2}(1+\cos\vartheta_{\mathbf{k},\mathbf{k}'}), \tag{4}$$

where D_{ac} is the acoustic phonon coupling constant, v_p is the sound speed in graphene, σ_m is the graphene areal density, and $\vartheta_{\mathbf{k},\mathbf{k}'}$ is the convex angle between $\mathbf{k}$ and $\mathbf{k}'$.

The electron-phonon matrix elements related to the longitudinal optical (LO), the transversal optical (TO) and the K phonons are (see for example [5])

$$\big|G^{(LO)}(\mathbf{k}',\mathbf{k})\big|^2 = \frac{1}{(2\pi)^2}\frac{\pi D_O^2}{\sigma_m\omega_O}\big(1-\cos(\vartheta_{\mathbf{k},\mathbf{k}'-\mathbf{k}}+\vartheta_{\mathbf{k}',\mathbf{k}'-\mathbf{k}})\big), \tag{5}$$

Table 1 Physical parameters for the scattering rates

σ_m	7.6×10^{-8} g/cm^2
v_F	10^6 m/s
v_p	2×10^4 m/s
D_{ac}	6.8 eV
$\hbar\omega_O$	164.6 meV
D_O	10^9 eV/cm
$\hbar\omega_K$	124 meV
D_K	3.5×10^8 eV/cm

$$\left|G^{(TO)}(\mathbf{k}',\mathbf{k})\right|^2 = \frac{1}{(2\pi)^2}\frac{\pi D_O^2}{\sigma_m \omega_O}\left(1 + \cos(\vartheta_{\mathbf{k},\mathbf{k}'-\mathbf{k}} + \vartheta_{\mathbf{k}',\mathbf{k}'-\mathbf{k}})\right), \tag{6}$$

$$\left|G^{(K)}(\mathbf{k}',\mathbf{k})\right|^2 = \frac{1}{(2\pi)^2}\frac{2\pi D_K^2}{\sigma_m \omega_K}(1 - \cos\vartheta_{\mathbf{k},\mathbf{k}'}), \tag{7}$$

where D_O is the optical phonon coupling constant, ω_O the optical phonon frequency, D_K is the K phonon coupling constant and ω_K the K phonon frequency. The angles $\vartheta_{\mathbf{k},\mathbf{k}'-\mathbf{k}}$ and $\vartheta_{\mathbf{k}',\mathbf{k}'-\mathbf{k}}$ denote the convex angles between $\mathbf{k}$ and $\mathbf{k}' - \mathbf{k}$ and between $\mathbf{k}'$ and $\mathbf{k}' - \mathbf{k}$, respectively.

In the literature there are several values for the coupling constants entering into the collision terms. For example for the acoustic deformation potential one can find values ranging from 2.6 eV to 29 eV. A similar degree of uncertainty is found for the optical and K phonon coupling constants as well. In our numerical simulations of monolayer graphene, the parameters proposed in [7, 8] have been adopted. They are reported in Table 1.

From the semiclassical transport equations, using a procedure developed for other semiconductors (see for example [9–14]), one can formulate macroscopic models that are more suited for CAD purposes because they avoid the numerical solutions of the Boltzmann equations, even if introduce some approximations for the needed closure relations, see e.g. [9, 15, 16].

Macroscopic quantities can be defined as moments of the distribution functions with respect to some suitable weight functions $\{\psi(\mathbf{k})\}$, assuming a sufficient regularity for the existence of the involved integrals. Of particular relevance are the following two moments

$$\text{average density} \quad \rho_i = \frac{4}{(2\pi)^2}\int_{\mathbb{R}^2} f_i(\mathrm{t},\mathbf{x},\mathbf{k})\,d\mathbf{k}, \tag{8}$$

$$\text{average velocity} \quad \rho_i \mathbf{V}_i = \frac{4}{(2\pi)^2}\int_{\mathbb{R}^2} f_i(\mathrm{t},\mathbf{x},\mathbf{k})\mathbf{v}\,d\mathbf{k} \tag{9}$$

(i = electrons, holes), where the factor 4 arises from taking into account both the spin states and the two equivalent valleys. The term $1/(2\pi)^2$ is the standard normalization of the elementary cell in the phase space for a two-dimensional crystal lattice [17].

By integrating the Boltzmann equations with respect to $\mathbf{k}$, one has the following balance equation involving the above-defined macroscopic quantities

$$\frac{\partial}{\partial t}\rho_i + \nabla_{\mathbf{x}} \cdot (\rho_i \mathbf{V}_i) = \rho_i C_i, \tag{10}$$

where the terms at the right hand sides are the density productions (the reader is referred to [16] for details).

If we introduce the current densities

$$\mathbf{J}_i = \mathsf{e}_i \rho_i \mathbf{V}_i, \quad i = e, h, \tag{11}$$

with e_i equal to $-e$ for electrons and e for holes, from Eqs. (10), one gets the celebrated drift-diffusion equations

$$\frac{\partial}{\partial t}(\mathsf{e}_i \rho_i) + \nabla_{\mathbf{x}} \cdot \mathbf{J}_i = \mathsf{e}_i (G - R), \quad i = e, h, \tag{12}$$

where the collision term $\mathsf{e}_i \rho_i C_i$ has been splitted as the sum of the generation and recombination terms G and R .

In Eq. (12) closure relations for the current and the recombination-generation terms must be prescribed. The classical approach models the currents as the sum of the diffusive and the drift part

$$\mathbf{J}_e = D_e \nabla_{\mathbf{x}} \rho_e + e \rho_e \mu_n \mathbf{E}, \tag{13}$$

$$\mathbf{J}_h = -D_h \nabla_{\mathbf{x}} \rho_h + e \rho_h \mu_p \mathbf{E}, \tag{14}$$

with the introduction of the diffusion coefficients D_i and the mobilities μ_i, $i = e, h$. If one considers as valid the Einstein relations, then $D_i = \mu_i k_B T$. The mobilities μ_i are assumed to be functions of the electric field and can parametrically depend also on other physical quantities. We will investigate their dependence on the Fermi level ε_F or equivalently on the electron density. Moreover we will assume that the mobility is isotropic that is it depends only on the modulus of the electric field E. Therefore we will take as mobility functional dependence

$$\mu_i = \tilde{\mu}_i(E, \rho_i). \tag{15}$$

More sophisticated models could take into account also a dependence on the lattice temperature and its gradient or the electron temperature.

In the sequel, as said, we will limit our analysis to the case of positive Fermi energies and therefore only the electrons contribute significantly to the current but it is straightforward to extend the analysis to holes as well.

In order to obtain the expression of the electron mobility, it is enough to consider the homogeneous case where

$$\mathbf{J}_e = e \rho_e \mu_n \mathbf{E}. \tag{16}$$

In the space-homogeneous case the Boltzmann equation relative to the K valley reduces to (we drop the valley and band indices for the sake of simplifying the notation)

$$\begin{aligned} \frac{\partial f(\mathrm{t}, \mathbf{k})}{\partial \mathrm{t}} - \frac{e}{\hbar} \mathbf{E} \cdot \nabla_{\mathbf{k}} f(\mathrm{t}, \mathbf{k}) = & \int S(\mathbf{k}', \mathbf{k}) f(\mathrm{t}, \mathbf{k}') \big(1 - f(\mathrm{t}, \mathbf{k})\big) \, d\mathbf{k}' \\ & - \int S(\mathbf{k}, \mathbf{k}') f(\mathrm{t}, \mathbf{k}) \big(1 - f(\mathrm{t}, \mathbf{k}')\big) \, d\mathbf{k}'. \end{aligned} \tag{17}$$

A similar equation holds for the K' valley. As initial condition we take the Fermi-Dirac distribution

$$f(0,\mathbf{k}) = \frac{1}{1+\exp(\frac{\varepsilon(\mathbf{k})-\varepsilon_F}{k_B T})},$$

where ε_F is the Fermi energy, which is related to the initial charge density by

$$\rho(0) = \frac{4}{(2\pi)^2}\int f(0,\mathbf{k})\,d\mathbf{k}. \tag{18}$$

As said, in (18) the factor 4 arises because we are considering both the two states of spin and the degeneracy (equal to 2) of the valley. As alternative one can consider the population of a single valley, and put equal to one the valley degeneracy and take in (18) $\rho(0)/2$ for the electron density. Note that in the unipolar case ρ remains constant, $\rho(\mathrm{t}) = \rho(0)$, as a consequence of the charge conservation.

If one fixes the electric field, the Fermi energy and the lattice temperature, as $\mathrm{t} \mapsto +\infty$ the solution of (17) gives the stationary distribution function which, inserted in relationship (9), allows us to evaluate $\mathbf{J}_e$. Therefore, if we are able to solve numerically the semiclassical Boltzmann equation, it is possible to get in a rather simple way the numerical values of the mobility as function of the electric field once the lattice temperature and Fermi energy have been assigned.

3 Application of the DG method to the electron transport equation in graphene

Lately several efficient numerical schemes have been applied for getting deterministic solutions of the Boltzmann equation for charge transport in semiconductors. Several works based on weighted essentially non oscillatory (WENO) schemes can be found in the literature about simulation of Silicon and Gallium Arsenide electron devices [18, 19] and recently also for suspended monolayer graphene [5]. Here we adopt the DG method for discretizing Eq. (17).

We choose a bounded domain $\Omega \subseteq \mathbb{R}^2$ such that $f(\mathrm{t},\mathbf{k}) \approx 0$ for every $\mathbf{k} \notin \Omega$ and $\mathrm{t} > 0$, and introduce a finite decomposition $\{C_\alpha\}_{\alpha=1}^N$ of Ω, with C_α appropriate open sets having a regular boundary, such that

$$C_\alpha \cap C_\beta = \emptyset \quad \text{if } \alpha \neq \beta, \text{ and } \bigcup_{\alpha=1}^{N} \overline{C_\alpha} = \Omega.$$

The distribution function is assumed to be constant in each cell C_α. If we denote by $\chi_\alpha(\mathbf{k})$ the characteristic function over the cell C_α, then the approximation of the distribution function f is given by

$$f(\mathrm{t},\mathbf{k}) \approx f^\alpha(\mathrm{t}) \quad \forall \mathbf{k} \in C_\alpha \quad \Longleftrightarrow \quad f(\mathrm{t},\mathbf{k}) \approx \sum_{\alpha=1}^{N} f^\alpha(\mathrm{t})\chi_\alpha(\mathbf{k}) \quad \forall \mathbf{k} \in \bigcup_{\alpha=1}^{N} C_\alpha.$$

This assumption replaces the unknown f, which depends on the two variables t and $\mathbf{k}$, with a set of N unknowns f^α, which depend only on time t. In order to obtain a set of N equations for the new unknowns f^α, we integrate Eq. (17) with respect to $\mathbf{k}$ over every cell

C_α and replace f with its approximation. The derivative of f with respect to the time is treated easily. We have

$$\int_{C_\alpha} \frac{\partial f(\mathrm{t},\mathbf{k})}{\partial \mathrm{t}}\, d\mathbf{k} \approx M_\alpha \frac{df^\alpha(\mathrm{t})}{d\mathrm{t}},$$

where M_α is the measure of the cell C_α. It is clear that the numerical method yields a system of ordinary differential equations by discretizing the collision operator and the drift term as discussed below. The final set of ordinary differential equations in time can be integrated by using a total variation diminishing (TVD) Runge-Kutta scheme [20].

3.1 Discretization of the collision operator

Since for each $\mathbf{k} \in C_\alpha$

$$\begin{aligned}
&\int S(\mathbf{k}',\mathbf{k}) f(\mathrm{t},\mathbf{k}')\big(1-f(\mathrm{t},\mathbf{k})\big)\, d\mathbf{k}' - \int S(\mathbf{k},\mathbf{k}') f(\mathrm{t},\mathbf{k})\big(1-f(\mathrm{t},\mathbf{k}')\big)\, d\mathbf{k}' \\
&\quad\approx \sum_{\beta=1}^{N} \left[\int_{C_\beta} S(\mathbf{k}',\mathbf{k}) f^\beta(\mathrm{t})\big(1-f^\alpha(\mathrm{t})\big)\, d\mathbf{k}' - \int_{C_\beta} S(\mathbf{k},\mathbf{k}') f^\alpha(\mathrm{t})\big(1-f^\beta(\mathrm{t})\big)\, d\mathbf{k}' \right] \\
&\quad= \sum_{\beta=1}^{N} \left[f^\beta(\mathrm{t})\big(1-f^\alpha(\mathrm{t})\big) \int_{C_\beta} S(\mathbf{k}',\mathbf{k})\, d\mathbf{k}' - f^\alpha(\mathrm{t})\big(1-f^\beta(\mathrm{t})\big) \int_{C_\beta} S(\mathbf{k},\mathbf{k}')\, d\mathbf{k}' \right],
\end{aligned}$$

if we define

$$A^{\alpha,\beta} = \int_{C_\alpha} \left[\int_{C_\beta} S(\mathbf{k},\mathbf{k}')\, d\mathbf{k}' \right] d\mathbf{k}, \tag{19}$$

we obtain

$$\begin{aligned}
&\int_{C_\alpha} \left[\int S(\mathbf{k}',\mathbf{k}) f(\mathrm{t},\mathbf{k}')\big(1-f(\mathrm{t},\mathbf{k})\big)\, d\mathbf{k}' - \int S(\mathbf{k},\mathbf{k}') f(\mathrm{t},\mathbf{k})\big(1-f(\mathrm{t},\mathbf{k}')\big)\, d\mathbf{k}' \right] d\mathbf{k} \\
&\quad\approx \sum_{\beta=1}^{N} \left[A^{\beta,\alpha}\big(1-f^\alpha(\mathrm{t})\big) f^\beta(\mathrm{t}) - A^{\alpha,\beta} f^\alpha(\mathrm{t})\big(1-f^\beta(\mathrm{t})\big) \right].
\end{aligned}$$

In doing so, the integral collision operator is replaced by quadratic polynomials. We note that the numerical coefficients $A^{\alpha,\beta}$ depend only on the scattering terms and the domain decomposition and can be evaluated analytically. The interested reader is referred to [21] for the detailed calculations.

3.2 Discretization of the drift term

We must approximate the term

$$-\frac{e}{\hbar}\mathbf{E} \cdot \int_{C_\alpha} \nabla_{\mathbf{k}} f(\mathrm{t},\mathbf{k})\, d\mathbf{k} = -\frac{e}{\hbar}\mathbf{E} \cdot \int_{\partial C_\alpha} f(\mathrm{t},\mathbf{k})\mathbf{n}\, d\sigma,$$

where $\mathbf{n}$ is the external unit normal to the boundary ∂C_α of the cell C_α. Since, due to the Galerkin method, the approximation of f is not defined on the boundary of the cells, we must introduce a *numerical flux*, that furnishes reasonable values of f on every ∂C_α,

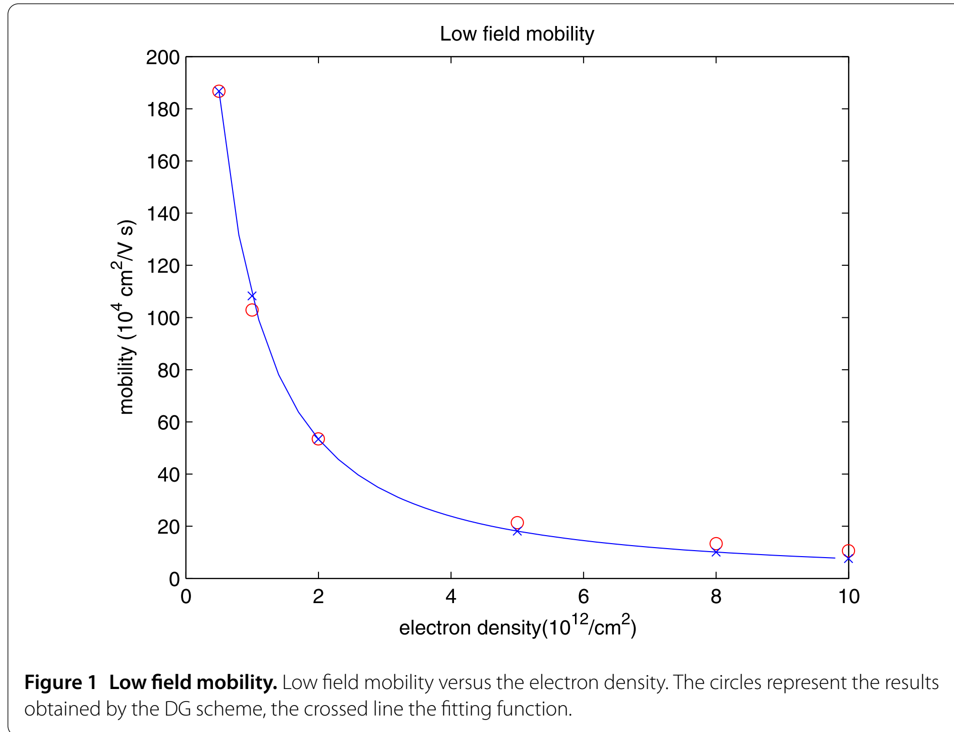

Figure 1 Low field mobility. Low field mobility versus the electron density. The circles represent the results obtained by the DG scheme, the crossed line the fitting function.

Table 2 Values of the fitting coefficients

ρ (10^{12}cm^{-2})	β_1	β_2	β_3	γ
0.5	2.5203	3.5728	1.0382	32.4631
1	2.7357	3.4656	1.1659	22.2200
2	3.1256	3.6552	1.1625	12.6928
5	2.0462	1.2446	1.2395	7.9534
8	1.7225	1.2159	1.2154	7.5381
10	1.7846	1.6393	1.2186	7.5336

depending on the values of the approximation of f in the nearest neighborhoods of the cell C_α and on the sign of $\mathbf{E} \cdot \mathbf{n}$. The simplest numerical flux is given by the *upwind rule*, that uses only the nearest adjacent cells. For the sake of shortness we refer the interested reader to [21, 22] for the details.

4 Electron mobility in monolayer graphene

By using the numerical scheme outlined in the previous section, we have numerically solved Eq. (17) and evaluated the electron mobility in monolayer graphene. The robustness and accuracy of the scheme has been investigated in [22], where a cross comparison with DSMC solutions has clearly validated both the approaches for a wide range of electric fields and Fermi energies.

The case of room lattice temperature (300 K) has been considered, for electron densities $\rho_e = 0.5, 1, 2, 5, 8, 10 \times 10^{12}/\text{cm}^2$. First of all, by extrapolation we have evaluated the low field mobility μ_0 defined as

$$\mu_0 = \lim_{E \mapsto 0^+} \mu(E, \rho).$$

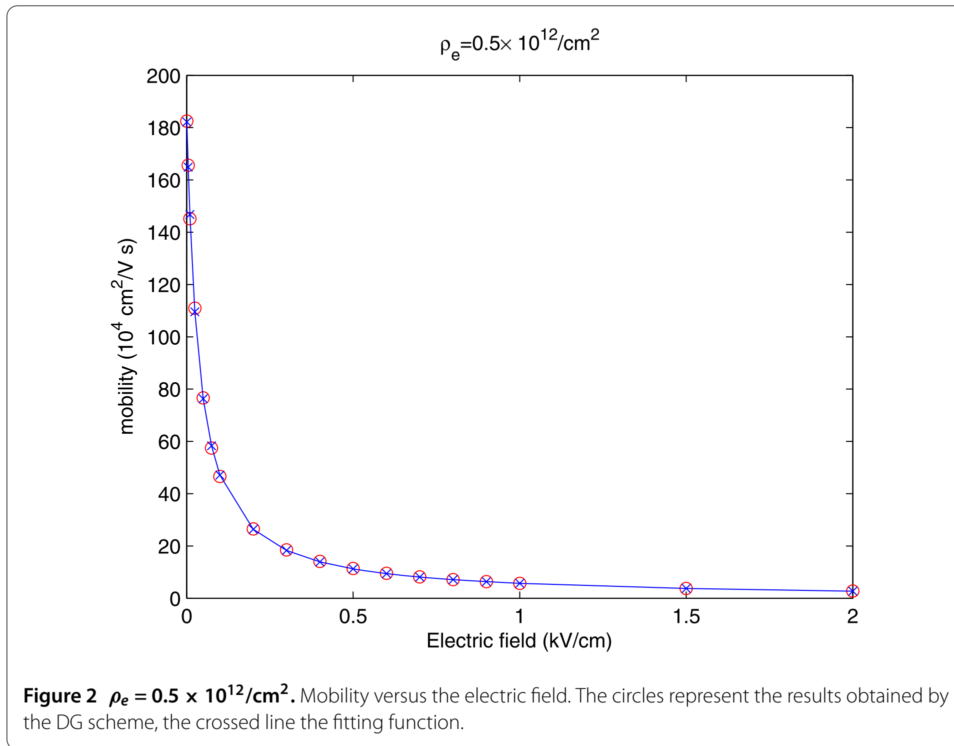

Figure 2 $\rho_e = 0.5 \times 10^{12}/\mathrm{cm}^2$**.** Mobility versus the electric field. The circles represent the results obtained by the DG scheme, the crossed line the fitting function.

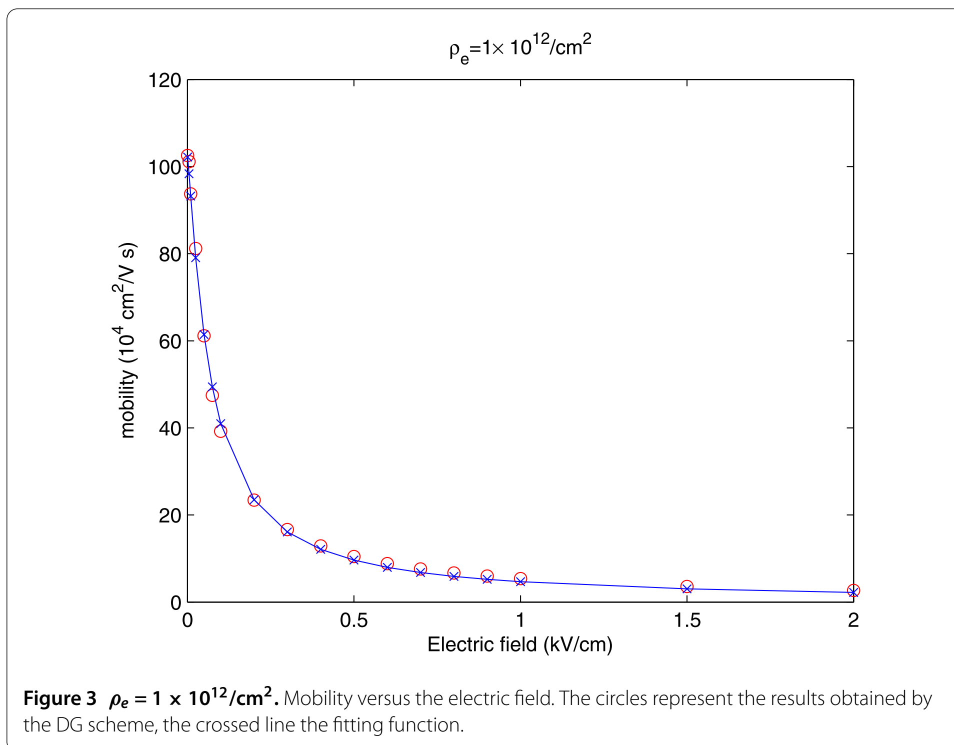

Figure 3 $\rho_e = 1 \times 10^{12}/\mathrm{cm}^2$**.** Mobility versus the electric field. The circles represent the results obtained by the DG scheme, the crossed line the fitting function.

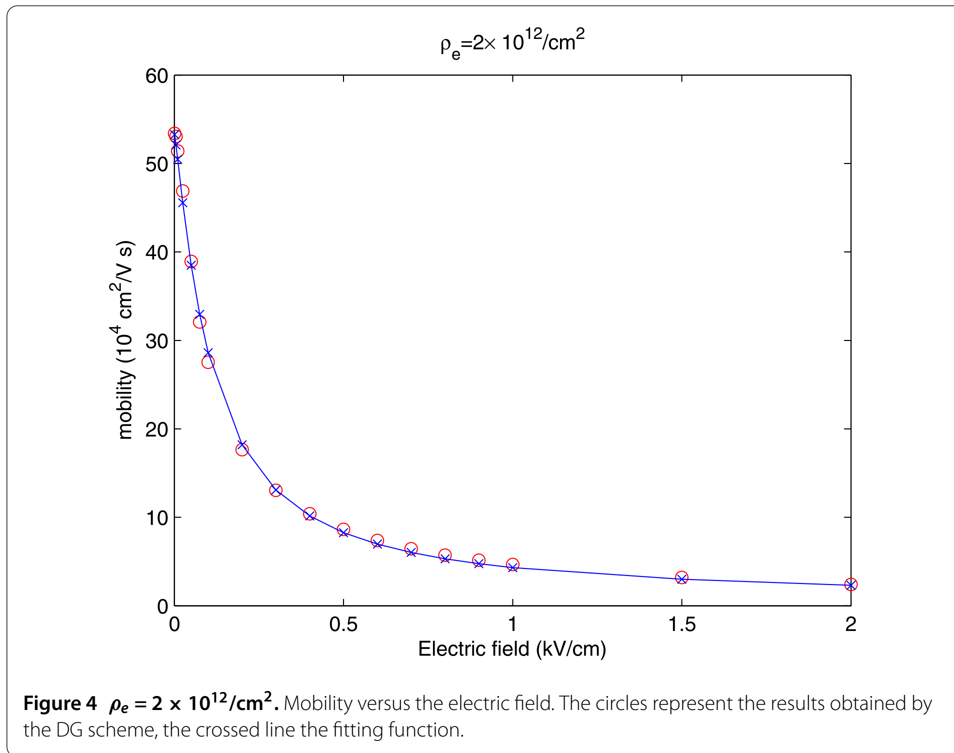

Figure 4 $\rho_e = 2 \times 10^{12}/\text{cm}^2$**.** Mobility versus the electric field. The circles represent the results obtained by the DG scheme, the crossed line the fitting function.

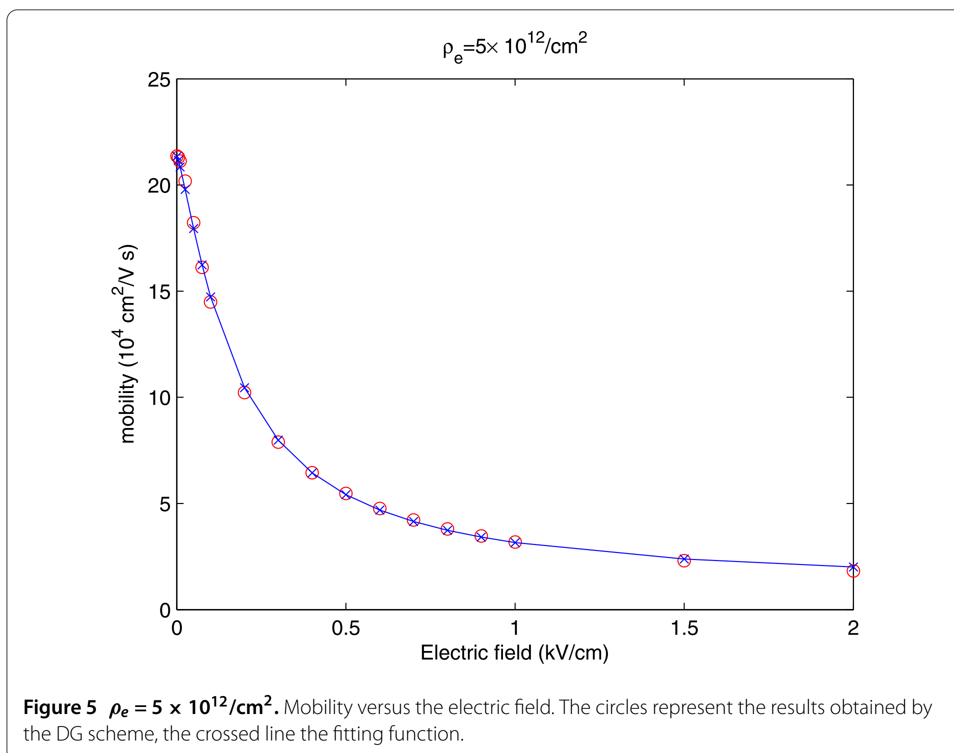

Figure 5 $\rho_e = 5 \times 10^{12}/\text{cm}^2$**.** Mobility versus the electric field. The circles represent the results obtained by the DG scheme, the crossed line the fitting function.

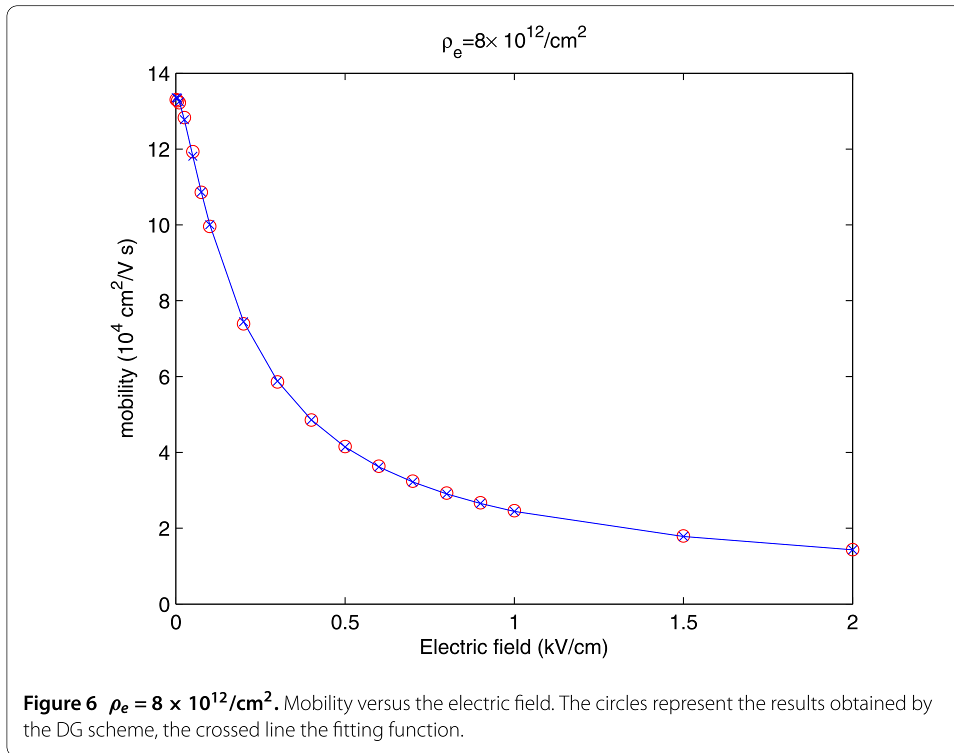

Figure 6 $\rho_e = 8 \times 10^{12}/\text{cm}^2$**.** Mobility versus the electric field. The circles represent the results obtained by the DG scheme, the crossed line the fitting function.

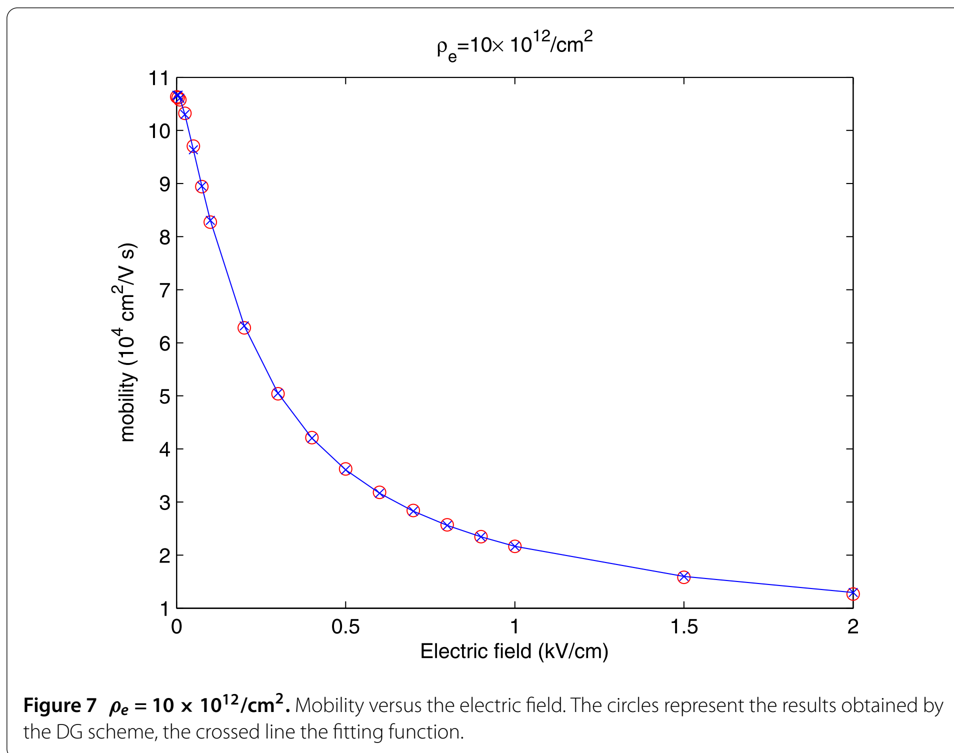

Figure 7 $\rho_e = 10 \times 10^{12}/\text{cm}^2$**.** Mobility versus the electric field. The circles represent the results obtained by the DG scheme, the crossed line the fitting function.

The results, reported in Figure 1, show that the low field mobility decreases with the rise of the carrier density as happens for graphene on SiO_2 [23]. The data are well fitted by the following empirical function, already used for Si device mobility [23],

$$\mu_0 = \mu_0(\rho) = \frac{\tilde{\mu}}{1 + (\rho/\rho_{ref})^{\alpha}}, \tag{20}$$

with $\rho_{ref} = 0.5 \times 10^{12}$ cm^{-2}, $\alpha = 1.2916$ and $\tilde{\mu} = 2\mu_0(\rho_{ref}) = 373.4306 \times 10^4$ cm^2/V s.

The low field mobility is then used in a formula, suitably adapted from that of Arora et al. [24], to fit the dependence of the mobility on the electric field at the considered values of the Fermi energy

$$\mu(E) = \frac{\mu_0 + \frac{v_F}{E}(\frac{E}{E_{ref}})^{\beta_1}}{1 + (\frac{E}{E_{ref}})^{\beta_2} + \gamma(\frac{E}{E_{ref}})^{\beta_3}}, \tag{21}$$

where $E_{ref} = 1$k V/cm and μ_0 is given by (20).

The values of the fitting coefficients are reported in Table 2. The data are well approximated for each value of ρ as can be seen from Figures 2-7.

Competing interests
The authors declare that they have no competing interests.

Authors' contributions
All authors have jointly worked to the manuscript with an equal contribution. All authors read and approved the final manuscript.

Author details
[1] Dipartimento di Matematica e Informatica, Università di Catania, Viale A. Doria 6, Catania, 95125, Italy. [2] Dipartimento di Matematica, Università della Calabria and INFN-Gruppo c. Cosenza, Via Ponte Bucci, Rende, Cosenza 87036, Italy.

Acknowledgements
The authors (AM and VR) acknowledge the financial support by the project FIR 2014 *Charge Transport in Graphene and Low dimensional Structures: modeling and simulation*, University of Catania, Italy. The author (GM) acknowledges the financial support from GNFM *Progetto giovani 2015*.

Received: 30 December 2015 Accepted: 18 July 2016 Published online: 02 August 2016

References
1. Castro Neto AH, Guinea F, Peres NMR, Novoselov KS, Geim AK. The electronic properties of graphene. Rev Mod Phys. 2009;81:109-62.
2. Selberherr S. Analysis and simulation of semiconductor devices. Berlin: Springer; 1984.
3. Cheng Y, Gamba IM, Majorana A, Shu C-W. A discontinuous Galerkin solver for Boltzmann-Poisson systems in nano devices. Comput Methods Appl Mech Eng. 2009;198:3130-50.
4. Cheng Y, Gamba IM, Majorana A, Shu C-W. A brief survey of the discontinuous Galerkin method for the Boltzmann-Poisson equations. Bol Soc Esp Mat Apl. 2011;56:47-64.
5. Lichtenberger P, Morandi O, Schürrer F. High-field transport and optical phonon scattering in graphene. Phys Rev B. 2011;84:045406.
6. Tomadin A, Brida D, Cerullo G, Ferrari AC, Polini M. Nonequilibrium dynamics of photoexcited electrons in graphene: collinear scattering, auger processes, and the impact of screening. Phys Rev B. 2013;88:035430.
7. Borysenko KM, Mullen JT, Barry EA, Paul S, Semenov YG, Zavada JM, Buongiorno Nardelli M, Kim KW. First-principles analysis of electron-phonon interactions in graphene. Phys Rev B. 2010;11:121412(R).
8. Li X, Barry EA, Zavada JM, Buongiorno Nardelli M, Kim KW. Surface polar phonon dominated electron transport in graphene. Appl Phys Lett. 2010;97:232105.
9. Mascali G, Romano V. A comprehensive hydrodynamical model for charge transport in graphene. In: IWCE-2014 Paris. 2014.
10. Alì G, Mascali G, Romano V, Torcasio CR. A hydrodynamical model for covalent semiconductors, with applications to GaN and SiC. Acta Appl Math. 2012;122(1):335.
11. Camiola VD, Mascali G, Romano V. Numerical simulation of a double-gate mosfet with a subband model for semiconductors based on the maximum entropy principle. Contin Mech Thermodyn. 2012;24(4–6):417.
12. Muscato O, Di Stefano V. An energy transport model describing heat generation and conduction in silicon semiconductors. J Stat Phys. 2011;144(1):171.

13. Barletti L. Hydrodynamic equations for electrons in graphene obtained from the maximum entropy principle. J Math Phys. 2014;55:083303.
14. Morandi O, Barletti L. Particle dynamics in graphene: collimated beam limit. J Comput Theor Transp. 2014;43:1-15.
15. Zamponi N, Barletti L. Quantum electronic transport in graphene: a kinetic and fluid-dynamical approach. Math Methods Appl Sci. 2011;34:807-18.
16. Camiola VD, Romano V. Hydrodynamical model for charge transport in graphene. J Stat Phys. 2014;157:11141137.
17. Jacoboni C. Theory of electron transport in semiconductors. Heidelberg: Springer; 2010.
18. Cáceres MJ, Carrillo JA, Majorana A. Deterministic simulation of the Boltzmann-Poisson system in GaAs-based semiconductors. SIAM J Sci Comput. 2006;27(6):1981-2009.
19. Galler M, Majorana A. Deterministic and stochastic simulations of electron transport in semiconductors. Bull Inst Math Acad Sin. 2007;2:349-65.
20. Shu C-W, Osher S. Efficient implementation of essentially non-oscillatory shock capturing schemes. J Comput Phys. 1988;77:439-71.
21. Coco M, Majorana A, Romano V. Cross validation of discontinuous Galerkin method and Monte Carlo simulations of charge transport in graphene on substrate. Ric Mat. 2016. doi:10.1007/s11587-016-0298-4.
22. Romano V, Majorana A, Coco M. DSMC method consistent with the Pauli exclusion principle and comparison with deterministic solutions for charge transport in graphene. J Comput Phys. 2015;302:267-84.
23. Dorgan VE, Bae M-H, Pop E. Mobility and saturation velocity in graphene on SiO_2. Appl Phys Lett. 2010;97:082112.
24. Arora ND, Hauser JR, Roulston DJ. Electron and hole mobilities in silicon as a function of concentration and temperature. IEEE Trans Electron Devices. 1982;29:292-5.

Submit your manuscript to a SpringerOpen journal and benefit from:

► Convenient online submission
► Rigorous peer review
► Immediate publication on acceptance
► Open access: articles freely available online
► High visibility within the field
► Retaining the copyright to your article

Submit your next manuscript at ► springeropen.com